Instrumentation Science and Technology, 41:535–544, 2013

ISSN: 1073-9149 print/1525-6030 online
DOI: 10.1080/10739149.2013.775590

AN OBLIQUE-INCIDENCE REFLECTIVITY DIFFERENCE STUDY OF THE DEPENDENCE OF PROBE-TARGET REACTION CONSTANTS ON SURFACE TARGET DENSITY USING STREPTAVIDIN-BIOTIN REACTIONS AS A MODEL

Yung-Shin Sun,[1,2] James P. Landry,[2] Yiyan Fei,[2] and Xiangdong Zhu[2]
[1]*Department of Physics, Fu-Jen Catholic University, New Taipei City, Taiwan*
[2]*Department of Physics, University of California at Davis, Davis, California, USA*

□ *A combination of the microarray platform and oblique-incidence reflectivity difference (OI-RD) microscopy was used to study the dependence of kinetic constants of probe-target reactions on the surface density of immobilized targets. Streptavidin-biotin reactions with a very high binding affinity were employed as the study model. Oblique-incidence reflectivity difference microscopy, a label-free and surface-based detection technique, was developed for monitoring real-time binding curves between two interactive biomolecules, enabling the acquisition of kinetic constants such as on-rate, off-rate, and equilibrium dissociation constants. These kinetic constants are important in characterizing biomolecular interactions because in living cells all intercellular and intermolecular reactions are at dynamic rather than at stable equilibrium. The kinetic constant of streptavidin binding to surface-immobilized biotin-bovine serum albumin was demonstrated to be significantly affected by the density of surface bovine serum albumin conjugates, mainly due to mass-transport effects within targets.*

Keywords biosensor, kinetics, label-free, reaction rates

INTRODUCTION

The microarray is a surface-based technique where various targets are immobilized on solid supports for reactions with solution-phase probes.[1] There are a number of advantages regarding such substrate-immobilized platforms. First, the sample consumption is very small, a crucial experimental consideration for studying protein-ligand interactions. Second, surface-immobilization on solid substrates supports the microarray

Address correspondence to Yung-Shin Sun, Department of Physics, Fu-Jen Catholic University, No.510, Zhongzheng Rd., Xinzhuang Dist., New Taipei City 24205, Taiwan (R.O.C.). E-mail: 089957@mail.fju.edu.tw

platform so that hundreds or thousands of biomolecular reactions can be followed simultaneously. Finally, it is noteworthy that in many (if not most) biomolecular interactions that occur *in vivo*, one of the participating reactants is often attached to a more or less immobile substrate or scaffold. However, as to the detection of biomolecular interactions, one should be mindful when comparing kinetic constants measured using bulk phase-based techniques such as isothermal titration calorimetry (ITC)[2–4] with those measured using surface immobilization-based platforms/techniques such as above-mentioned microarray and surface plasma resonance (SPR).[5–7] In a reaction between solution-phased probes and surface-immobilized targets, the mass transport of the probe to the surface of the solid support and through the matrix of the target layer to its actual binding partners affects the measured kinetic constants.[8,9] The effect of mass transport through the solution to the solid surface can be minimized by having the probe solution flow along the surface at suitable rates. On the other hand, the mass transport of probes through the target layer to the specific binding partners (epitopes or ligands) is dependent on the structural details (and indirectly on the density) of the immobilized targets. Target density affects both the efficiency and binding kinetics of DNA-DNA hybridization as described elsewhere.[10,11] When the target layer involves polymers, commonly used to increase the total amount of available targets per unit area, the binding curves are seriously affected by mass transport of the probes through the polymer. This is the case as dextran matrixes are routinely used in SPR-based detection.[12]

Because of the difficulties in precisely controlling the amounts of surface-immobilized targets, few experiments have been conducted to systemically reveal and study such mass-transport effects on reaction constants.[12–14] In this article, using a combination of microarray platform and oblique-incidence reflectivity difference (OI-RD) microscopy, we studied the dependence of the kinetic constants on the density of surface-immobilized targets. By controlling the printing concentration, microarray spots with different amounts of targets were fabricated. The density of these spots was compared with those of mono-layered proteins after the blocking step of a standard microarray protocol.[15] The microarray was reacted with a specific probe for acquiring the binding curves as well as the kinetic constants of a set of probe-target reactions. The dependence of the binding constants on the density of surface targets was studied, as a result of mass-transport effects. In addition, the binding affinities measured with an OI-RD microscope were compared with those measured with a commercial SPR-based instrument, BIAcore 3000, under the same reaction conditions.

MATERIALS AND METHODS

Protein Probes and Ligand Targets

Unlabeled streptavidin tetramers were purchased from Jackson ImmunoResearch Laboratories (West Grove, PA). They were dissolved in 1 × PBS (Phosphate-buffered saline) as protein probes against biotin. Biotin and bovine serum albumin (BSA) were purchased from Sigma Aldrich (St. Louis, MO) and used as received. To conjugate biotin molecules on the BSA scaffolds, 0.5 mL of N-hydroxysuccinimide ester (NHS) of biotin (0.23 μmole) solution in dimethyl sulfoxide was added into a 5 mL solution of BSA (0.0058 μmole) in 0.1 M $NaHCO_3$ and rotated in a plastic tube overnight. Biotinylated BSA was precipitated by adding 25 mL of ethanol, filtered and washed with ethanol and acetonitrile three times, respectively, and then dissolved in 5 mL of pure water and lyophilized. Only a fraction of all 35 amine residues on a BSA molecule were conjugated to biotin molecules, and the rest of them were used for immobilization on epoxy-coated substrates.

Preparation of Target Microarrays and Procedure of Subsequent Reactions

Biotin-BSA conjugates were dissolved in 1 × PBS and further diluted into printing solutions at concentrations decreasing successively by a factor of 0.75 from 15.2 to 0.64 μM. Two copies of each of the 12 concentrations were printed into microarrays on epoxy-coated glass slides (CEL Associates, Pearland, TX) with an OmniGrid 100 contact-printing arrayer (Digilab, Holliston, MA). Unmodified BSA at a concentration of 8.3 μM was also printed as a negative control. The microarray-bearing slides were stored as printed in slide boxes for at least 24 hr before further processing. Afterward, the slide was assembled into a flow chamber and washed twice with a flow of 1 × PBS at a flow rate of 30 mL/min. To block the remaining free epoxy groups on the glass surface from non-specific reaction with protein probes, we exposed the printed surface to a flowing BSA solution at 8.3 μM in 1 × PBS for 10 min and then washed the surface with a flow of 1 × PBS for 5 min. For the probe reaction, we replaced 1 × PBS buffer in the flow chamber with a solution of 100 nM streptavidin at a flow rate of 30 mL/min for a few seconds and then reduced the flow rate to 0.05 mL/min during the remainder of the reaction.

OI-RD Scanning Microscope for Label-Free Detection of Protein-Ligand Reactions

The oblique-incidence reflectivity difference (OI-RD) scanning microscope used in the present work was described in an earlier publication.[16]

It employed a He-Ne laser at a wavelength (λ) of 633 nm for illumination. We measured the complex differential reflectivity change ($\Delta_p - \Delta_s$) across a microarray-covered glass surface.[17] The physical properties of a surface-bound molecular layer on a glass surface are related to $\Delta_p - \Delta_s$ by[15,18,19]

$$\Delta_p - \Delta_s \cong -i\left[\frac{4\pi\varepsilon_s(\tan\varphi_{inc})^2\cos\varphi_{inc}}{\varepsilon_0^{1/2}(\varepsilon_s-\varepsilon_0)\left(\varepsilon_s/\varepsilon_0-(\tan\varphi_{inc})^2\right)}\right] \times \frac{(\varepsilon_d-\varepsilon_s)(\varepsilon_d-\varepsilon_0)\Theta}{\varepsilon_d}\left(\frac{d}{\lambda}\right), \quad (1)$$

where φ_{inc} is the incident angle of illumination, ε_0, ε_d, and ε_s are the respective optical constants of aqueous ambient, the molecular layer (e.g., captured protein probes), and the glass slide at $\lambda = 633$ nm, d is the thickness of the molecular layer, and Θ is the coverage of the layer, defined as the ratio of the area covered by the layer to the total available area. In this present article, $\varphi_{inc} = 65°$, $\varepsilon_s = 2.307$ for glass slide, $\varepsilon_0 = 1.788$ for aqueous buffer, and $\varepsilon_d = 2.031$ for proteins in solution.[15]

An image of a microarray was acquired with pixel dimensions of 20 μm × 20 μm. To acquire binding curves, we selected one pixel from a printed spot (target pixel) and one pixel from the unprinted region adjacent to the printed target (reference pixel) and measured the optical signals from these pixels at a time interval shorter than the characteristic time of the reaction. We took the difference between the signal of a target pixel and the signal of its reference pixel as the binding curve. This significantly reduced the contribution of the drift in the optical system to the measurement.

SPR-Based Measurements

For SPR-based measurements, a BIAcore 3000 device with an auto-sampler and CM5 (carboxylate dextran matrix) chips was used (Uppsala, Sweden). The immobilization of biotin-BSA conjugates was performed at 25°C using HBS-P (10 mM Hepes, 150 mM NaCl, pH 7.4, and 0.005% polyoxyethylene (20) sorbitan monooleate [P-20]) as the running buffer. The surface was first activated by a 200 μL injection of 1:1 mixed 50 mM NHS and 200 mM EDC (3-(*N*,*N*-dimethylamino)propyl-N-ethylcarbodiimide). Then 100 μL of biotin-BSA solution (3.3 μM in 10 mM sodium acetate, pH 4.0) was injected at a flow rate of 10 μL/min. Subsequently, the surface was blocked by injecting 100 μL of 1 M ethanolamine (pH 8.5), which deactivated residual reactive sites. For kinetic measurements, running buffer (1 × PBS, pH 7.4) was first injected at a flow rate of

10 μL/min for 1 min, and then streptavidin (100 nM in 1 × PBS) was injected at the same rate for 30 min.

RESULTS AND DISCUSSION

Biotin-BSA conjugates were immobilized on epoxy-coated substrates via covalent epoxy-amine chemistry. Streptavidin binds to biotin through hydrogen bonds and such binding is known as one of the strongest non-covalent interactions in nature. From left to right, Figure 1(A) shows the microarray image after washing with 1 × PBS, the image after blocking with BSA, and the image after reaction with streptavidin. The spot size was around 130 μm in diameter, and the center-to-center spacing was about 250 μm. After washing, all target spots were visible and the OI-RD signal was proportional to the printing concentration. In this case, BSA molecules were immobilized on the epoxy-coated surface as depicted in the top cartoon of Figure 1(B). From the lowest to the highest printing concentration, less than a "side-on" monolayer, a "side-on" monolayer, a mixed "side-on" and "end-on" monolayer, an "end-on" monolayer, and more than an "end-on" monolayer of BSA molecules were immobilized on the surface.[15] After blocking, free BSA molecules were bound to unprinted (background) regions, and all target spots became darker since the background signal increased. It has been shown that under this blocking concentration (8.3 μM of BSA), a "side-on" monolayer of fully packed BSA

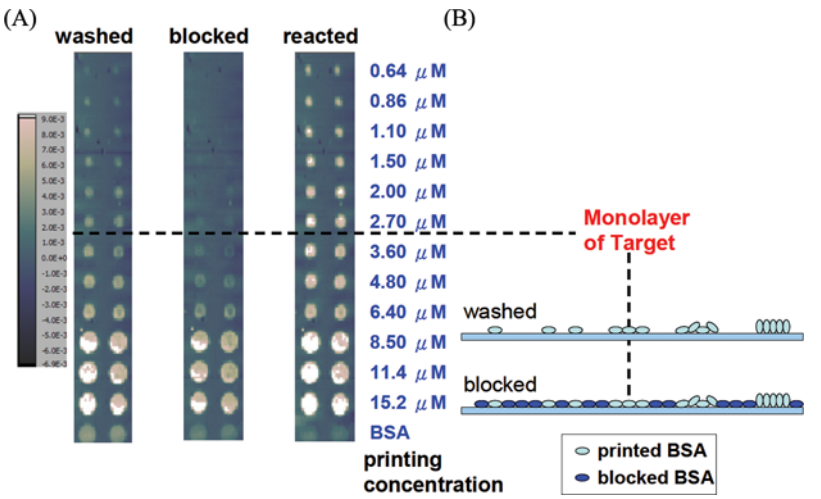

FIGURE 1 (A) From left to right: the microarray image after washing with 1 × PBS, the image after blocking with 8.3 μM of BSA, and the image after reaction with 100 nM of streptavidin. (B) Schematic depiction of the blocking process. (color figure available online.)

molecules was accumulated on the surface. Therefore, for those spots not visible after blocking, they must have less than a "side-on" monolayer of fully packed BSA molecules printed on the surface. As shown in the bottom cartoon of Figure 1(B), the first three spots were not visible since their printed BSA molecules are equal to or less than the surrounding blocked BSA molecules (which corresponds to a "side-on" monolayer). It is useful to apply such blocking steps to determine the amount of printed molecules having more or less the same sizes as BSA. In the present article, it is concluded that at printing concentrations between 2.7 and 3.6 μM, a "side-on" monolayer of BSA molecules could be immobilized on the surface. After reaction, all spots except BSA light up due to streptavidin binding to surface biotin-BSA conjugates. The corresponding association curves are shown in Figure 2(A). It is clear that the OI-RD signal increases as the printing concentration increases simply because of more available biotin molecules on the surface. Each curve is fitted to the simple Langmuir model,[16,20]

$$OI - RD\ Signal\ \alpha[1 - \exp(-k_{on}[c]t)], \tag{2}$$

assuming $k_{off} = 0$ since streptavidin-biotin binding is very strong with almost no dissociation.[21] Figure 2(B) shows the "reaction rate" (in k_{on}[c], [c] is the probe concentration) and change in OI-RD signal versus printing concentration as a result of streptavidin binding to biotin-BSA targets. The dashed line corresponds to the printing concentration (around 3 μM) where a "side-on" monolayer of BSA molecules was immobilized on the surface. There is a sudden drop in the reaction rate at a printing concentration near 3 μM ($k_{on}[c] = 0.02 \sim 0.03\,s^{-1}$ at printing concentrations less than 3 μM; $k_{on}[c] = 0.005 \sim 0.015\,s^{-1}$ at printing concentrations higher than 3 μM), indicating that the on-rate (k_{on}) decreases because of excess surface BSA molecules and the subsequently occurring mass-transport effect. The on-rate at a printing concentration of 1 μM was about $4 \sim 5$ times larger than that at 15 μM. These results suggest that the reaction rate would be most accurate at printing concentrations less than a certain value where near (or less than) a monolayer of targets is immobilized. Once the printing concentration is high enough to form a multilayer, the reaction rate would be much smaller since it takes time for more probes to penetrate into deeper layers and to react with those underneath targets.

Figure 3 shows the association curves of streptavidin binding to surface-immobilized biotin-BSA conjugates measured with an OI-RD microscope and an SPR-based BIAcore 3000. For OI-RD detection, biotin-BSA at 8.3 μM was printed on epoxy-coated glass slides; while in SPR measurement, biotin-BSA at 3.3 μM was immobilized on CM5 chips. Subsequently, streptavidin at 100 nM was reacted with surface biotin-BSA conjugates in both

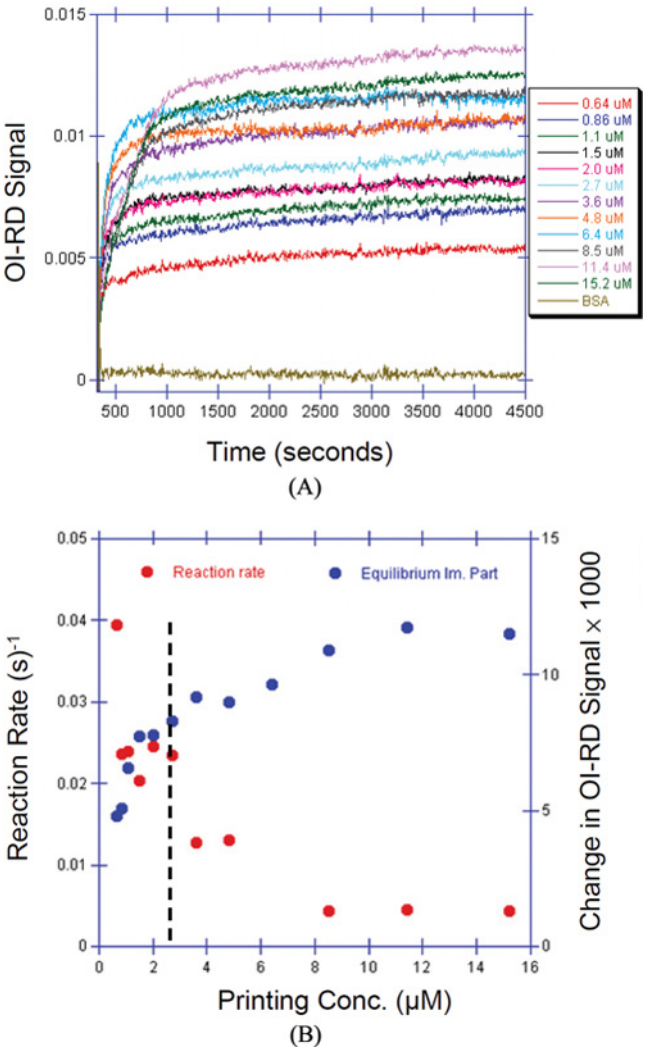

FIGURE 2 (A) Association curves of streptavidin at 100 nM reacting with surface-immobilized biotin-BSA conjugates at different printing concentrations. To acquire the reaction rate, each curve was fitted to the simple Langmuir model. (B) Reaction rate (k_{on}[c]) and change in OI-RD signal versus printing concentration due to streptavidin binding to biotin-BSA targets at different printing concentrations. (color figure available online.)

cases under the same conditions. Both OI-RD and SPR signals were converted into surface mass density for comparison (see reference[15] for OI-RD conversion and 1 RU $\sim$ 1 pg/mm^2 of surface-immobilized biomolecules for SPR conversion[22]). The mass density of bound streptavidin near equilibrium is higher in the SPR measurement (15 ng/mm^2 at 1200 s) than in OI-RD detection (11.5 ng/mm^2 at 1200s), which is simply due to the

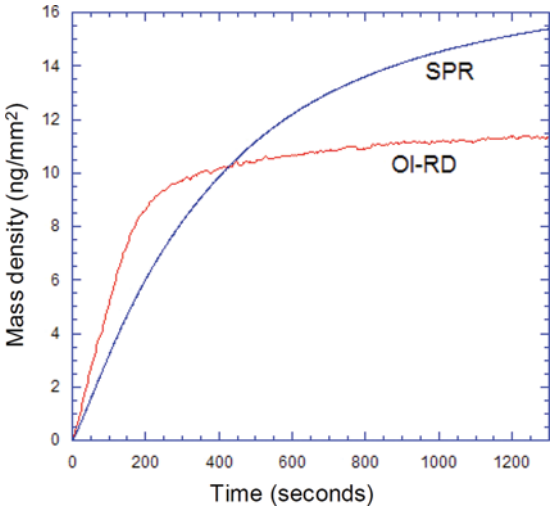

FIGURE 3 Comparison of real-time binding curves between an OI-RD microscope and an SPR-based instrument. For OI-RD detection, biotin-BSA at 8.3 μM was printed on epoxy-coated glass slides; in SPR measurements, biotin-BSA at 3.3 μM was immobilized on CM5 chips. Streptavidin at 100 nM was reacted with surface biotin-BSA conjugates in both cases. (color figure available online.)

difference in the amount of immobilized biotin-BSA conjugates. Commercial SPR-based instruments are designed to detect a very tiny amount of probes (i.e., either the concentration or the molecular weight of the probe is very low), so the chip surface is functionalized and processed for capturing as many targets as possible. After fitting these 2 curves to the simple Langmuir model, the reaction rate (k_{on}[c]) derived from OI-RD detection ($6.7 \times 10^{-3}\,s^{-1}$) was almost three times larger than that drawn from SPR measurement ($2.3 \times 10^{-3}\,s^{-1}$). This is the result of excess multi-layered targets where mass-transport effect stays dominant. While SPR-based measurements have very high sensitivities, the derived reaction rates using a simple fitting model may be uncertain. To overcome this defect to a certain extent, one can fit kinetic curves with different models such as the simple Langmuir model with mass-transport effect taken into consideration or the sophisticated two-site Langmuir model.[20,23,24]

CONCLUSIONS

We studied the dependence of kinetic constants on the density of surface-immobilized targets using a combination of a microarray platform and an oblique-incidence reflectivity difference (OI-RD) microscope. It is suggested that, in the current microarray platform, BSA blocking is a practical step to effectively determine the amount (or density) of

surface-immobilized biomolecules compared to a mono-layered proteins. The results also indicated that the reaction slowed down when there were excess (more than a "side-on" monolayer of) targets immobilized on the surface. Although increasing the amount of surface targets boosts the number of captured probes, and thus the detected signals, the inaccuracy in derived reaction rates should be considered as an undesirable trade-off.

ACKNOWLEDGMENTS

The authors thank financial support from NIH-R01-HG003827 (X. D. Zhu) and Taiwan NSC 101-2112-M-030-003-MY3 (Y. S. Sun).

REFERENCES

1. Schena, M. *Microarray Analysis*; Wiley: Hoboken, NJ, 2003.
2. Krainer, G.; Broecker, J.; Vargas, C.; Fanghanel, J.; Keller, S. Quantifying high-affinity binding of hydrophobic ligands by isothermal titration calorimetry. *Analyt. Chem.* **2012**, *84*(24), 10715–10722.
3. Parker, K. M.; Stalcup, A. M. Affinity capillary electrophoresis and isothermal titration calorimetry for the determination of fatty acid binding with beta-cyclodextrin. *J. Chromatogr. A* **2008**, *1204*(2), 171–182.
4. Talhout, R.; Villa, A.; Mark, A. E.; Engberts, J. B. F. N. Understanding binding affinity: A combined isothermal titration calorimetry/molecular dynamics study of the binding of a series of hydrophobically modified benzamidinium chloride inhibitors to trypsin. *J. Amer. Chem. Soc.* **2003**, *125*(35), 10570–10579.
5. Gonzalez-Fernandez, E.; de-los-Santos-Alvarez, N.; Miranda-Ordieres, A. J.; Lobo-Castanon, M. J. SPR evaluation of binding kinetics and affinity study of modified RNA aptamers towards small molecules. *Talanta* **2012**, *99*, 767–773.
6. Rispens, T.; Te Velthuis, H.; Hemker, P.; Speijer, H.; Hermens, W.; Aarden, L. Label-free assessment of high-affinity antibody-antigen binding constants. Comparison of bioassay, SPR, and PEIA-ellipsometry. *J. Immunolog. Meth.* **2011**, *365*(1–2), 50–57.
7. Zakhary, D. R.; Bond, M. Differences is the RII-binding domains or AKAPs regulate affinity of RII binding: analysis by SPR. *Biophys. J.* **2000**, *78*(1), 432a.
8. Sigmundsson, K.; Masson, G.; Rice, R. H.; Beauchemin, N.; Obrink, B. Determination of active concentrations and association and dissociation rate constants of interacting biomolecules: An analytical solution to the theory for kinetic and mass transport limitations in biosensor technology and its experimental verification. *Biochemistry* **2002**, *41*(26), 8263–8276.
9. Jennissen, H. P.; Zumbrink, T. Mass transport-free protein adsorption kinetics in biosensor systems. *Faseb J.* **2001**, *15*(4), A531.
10. Peterson, A. W.; Wolf, L. K.; Georgiadis, R. M. Hybridization of mismatched or partially matched DNA at surfaces. *J. Amer. Chem. Soc.* **2002**, *124*(49), 14601–14607.
11. Michel, W.; Mai, T.; Naiser, T.; Ott, A. Optical study of DNA surface hybridization reveals DNA surface density as a key parameter for microarray hybridization kinetics. *Biophys. J.* **2007**, *92*(3), 999–1004.
12. Rich, R. L.; Myszka, D. G. Advances in surface plasmon resonance biosensor analysis. *Curr. Opin. Biotechnol.* **2000**, *11*(1), 54–61.
13. Karlsson, R.; Falt, A. Experimental design for kinetic analysis of protein-protein interactions with surface plasmon resonance biosensors. *J. Immunol. Meth.* **1997**, *200*(1–2), 121–133.
14. O'Shannessy, D. J. Determination of kinetic rate and equilibrium binding constants for macromolecular interactions: a critique of the surface plasmon resonance literature. *Curr. Opin. Biotechnol.* **1994**, *5*(1), 65–71.

15. Landry, J. P.; Sun, Y. S.; Guo, X. W.; Zhu, X. D. Protein reactions with surface-bound molecular targets detected by oblique-incidence reflectivity difference microscopes. *Appl. Opt.* **2008**, *47*(18), 3275–3288.
16. Sun, Y. S.; Landry, J. P.; Fei, Y. Y.; Zhu, X. D.; Luo, J. T.; Wang, X. B.; Lam, K. S. Effect of fluorescently labeling protein probes on kinetics of protein-ligand reactions. *Langmuir* **2008**, *24*(23), 13399–13405.
17. Thomas, P.; Nabighian, E.; Bartelt, M. C.; Fong, C. Y.; Zhu, X. D. An oblique-incidence optical reflectivity difference and LEED study of rare-gas growth on a lattice-mismatched metal substrate. *Appl. Phys. A* **2004**, *79*, 131–137.
18. Zhu, X.; Landry, J. P.; Sun, Y. S.; Gregg, J. P.; Lam, K. S.; Guo, X. Oblique-incidence reflectivity difference microscope for label-free high-throughput detection of biochemical reactions in a microarray format. *Appl. Opt.* **2007**, *46*(10), 1890–1895.
19. Zhu, X. D. Oblique-incidence optical reflectivity difference from a rough film of crystalline material. *Phys. Rev. B* **2004**, *69*(115407), 1–5.
20. Morton, T. A.; Myszka, D. G.; Chaiken, I. M. Interpreting complex binding kinetics from optical biosensors: a comparison of analysis by linearization, the integrated rate equation, and numerical integration. *Anal. Biochem.* **1995**, *227*(1), 176–185.
21. Chen, H. M.; Huang, T. H.; Tsai, R. M. A biotin-hydrogel-coated quartz crystal microbalance biosensor and applications in immunoassay and peptide-displaying cell detection. *Anal. Biochem.* **2009**, *392*(1), 1–7.
22. Balamurugan, S.; Obubuafo, A.; McCarley, R. L.; Soper, S. A.; Spivak, D. A. Effect of linker structure on surface density of aptamer monolayers and their corresponding protein binding efficiency. *Anal. Chem.* **2008**, *80*(24), 9630–9634.
23. Campagnolo, C.; Meyers, K. J.; Ryan, T.; Atkinson, R. C.; Chen, Y. T.; Scanlan, M. J.; Ritter, G.; Old, L. J.; Batt, C. A. Real-Time, label-free monitoring of tumor antigen and serum antibody interactions. *J. Biochem. Biophys. Meth.* **2004**, *61*(3), 283–298.
24. Heding, A.; Gill, R.; Ogawa, Y.; De Meyts, P.; Shymko, R. M. Biosensor measurement of the binding of insulin-like growth factors I and II and their analogues to the insulin-like growth factor-binding protein-3. *J. Biol. Chem.* **1996**, *271*(24), 13948–13952.